**Mohammad Sharif Shourijeh**
Mechanical Engineering Department,
University of Ottawa,
Ottawa, ON K1N 6N5, Canada
e-mail: msharifs@uottawa.ca

**Reza Sharif Razavian**
Department of Systems Design Engineering,
University of Waterloo,
Waterloo, ON N2L-3G1, Canada
e-mail: rsharifr@uwaterloo.ca

**John McPhee**
Department of Systems Design Engineering,
University of Waterloo,
Waterloo, ON N2L-3G1, Canada
e-mail: mcphee@uwaterloo.ca

# Estimation of Maximum Finger Tapping Frequency Using Musculoskeletal Dynamic Simulations

*A model for forward dynamic simulation of the rapid tapping motion of an index finger is presented. The finger model was actuated by two muscle groups: one flexor and one extensor. The goal of this analysis was to estimate the maximum tapping frequency that the index finger can achieve using forward dynamics simulations. To achieve this goal, each muscle excitation signal was parameterized by a seventh-order Fourier series as a function of time. Simulations found that the maximum tapping frequency was 6 Hz, which is reasonably close to the experimental data. Amplitude attenuation (37% at 6 Hz) due to excitation/activation filtering, as well as the inability of muscles to produce enough force at high contractile velocities, are factors that prevent the finger from moving at higher frequencies. Musculoskeletal models have the potential to shed light on these restricting mechanisms and help to better understand human capabilities in motion production.*
[DOI: 10.1115/1.4036288]

## 1 Introduction

Finger tapping is a common motion in a variety of daily activities, such as playing musical instruments, typing on a keyboard, and tapping on smart phones. However, very few studies have addressed this movement [1,2]. Specifically, no dynamical analysis of fast and repetitive finger tapping, and the associated musculotendon demands, has been reported before. The dynamical analysis of finger tapping motion can help researchers to study conditions such as repetitive strain injury and the underlying mechanisms.

Human voluntary motions are produced by muscle contractions that are created by muscle activations. In modeling of the human movements, one should solve a problem where the number of unknowns (muscle activation levels) is greater than the number of degrees-of-freedom (DOF). This problem is usually referred to as the muscle redundancy problem in musculoskeletal system modeling, for which there is no unique solution. To pick one solution out of the many possible solutions, extra criteria should be considered. A common practice is to search for a solution that minimizes a physiological index through an optimization process.

When the goal is to find the optimal time-history of a signal (e.g., muscle forces or activations through the course of an action) one must solve an optimal control problem (OCP). In Refs. [3–5], several classical approaches for solving a general optimal control problem are presented, including linear quadratic regulator (LQR) control, linear quadratic Gaussian (LQG) control, variational approaches such as direct collocation (DC), model predictive control (MPC), and parameterization. For all techniques, pros and cons are involved. It should be noted that not all of those approaches are applicable to musculoskeletal modeling; for instance, the analytical solution in Ref. [6] belongs to the cases with submaximal contractions only, and LQR and LQG are for linear systems. The MPC normally works in linear or linearized systems with quadratic optimization form only, and DC requires a complicated implementation and has been scarcely applied recently [7–9]. Hierarchical optimal control methods [10–13] have also been used for optimal control of musculoskeletal systems; the drawback of these methods is the complexity associated with the dynamical consistency between multiple levels of control.

Dynamic optimization (DO, also known as the "shooting method" in the optimal control literature [14]), in spite of high computation cost, might result in more realistic outcomes as it considers all the time-course in the optimization procedure and solves for the time-history of the decision signals [15–17]. Therefore, in contrast to static optimization (SO) [18–23], DO takes into account the effect of previous time instants on the current instant of simulation.

Local parameterization has been used by a few researchers, e.g., Ackermann [15] and Garcia-Vallejo and Schiehlen [24]. Locally parameterizing the control signals or state variables sounds like a promising approach, as it captures the local dynamics of the system as long as the time-windows are small enough. However, by increasing the number of parameterization windows, the scale of the optimization problem, and therefore, the computation time, increase significantly.

Using a control signal parameterization method, by means of parametric pattern functions as the control inputs, the OCP can be converted to a nonlinear optimization problem. Different parameterization functions might be used, based on the information of the system, degree of nonlinearity, and a priori data. Global and local parameterizations might be utilized. For instance, different types of functions can be used for the global control parameterization, such as Fourier series [17,25–27] or local functions within finite windows of the simulation using splines [24]. Although global parametrization, compared to local parameterization, may miss some local dynamics of the system, this approach will provide good suboptimal results in general. Also, for applications with no drastic changes in the control signals (a priori knowledge of the system behavior is required), global parameterization will output reasonable results. In addition, global parameterization will reduce the number of decision variables considerably and also does not require continuity constraints at the control nodes, which results in significant reduction of the computation time.

In this paper, we present a forward dynamics analysis of finger tapping motion. The relevant works in this area are reported in Refs. [1] and [2], where the musculotendon demand is studied using an inverse dynamic simulation. The advantage of forward dynamics simulation over inverse dynamics is that it can be used when no measured kinematic data are available. Forward

Contributed by the Design Engineering Division of ASME for publication in the Journal of Computational and Nonlinear Dynamics. Manuscript received April 13, 2016; final manuscript received February 21, 2017; published online May 4, 2017. Assoc. Editor: Arend L. Schwab.


Copyright © 2017 by ASME

Downloaded From: http://computationalnonlinear.asmedigitalcollection.asme.org/ on 01/15/2018 Terms of Use: http://www.asme.org/about-asme/terms-of-use

dynamics simulations enable us to study motions that are beyond the biological limits of the system, or conduct what-if scenarios to support design optimization and ergonomics.

The goal of this study is to develop and present a musculoskeletal model for the index finger to investigate the dynamics of a fast tapping movement and to estimate the maximum tapping frequency. For this purpose, we have used dynamic optimization using a global parameterization to solve the optimal control problem.

## 2 Finger Tapping Musculoskeletal Model

In this section, the musculoskeletal model for forward dynamic simulation of the rapid finger tapping motion is presented. The model consists of a rigid index finger rotating around the metacarpophalangeal joint (e.g., a 1DOF pendulum, see Fig. 1) with two muscle groups: one as flexor and the other as extensor.

The muscle model is a three-element Hill model based on Ref. [28]. The activation and contraction dynamics expressions employed for this model are presented in the Appendix.

The following assumptions are made for the finger modeling and simulation:

(1) The maximum isometric force parameter $F_{\max}$ is calculated by multiplying the physiological cross-sectional area (PCSA) with the muscle specific tension. The effective extensor PCSA is assumed to be the sum of the extensor digitorum communis (EDC) and the extensor indicis proprius (EIP) PCSAs. The effective flexor PCSA is assumed to be the sum of the flexor digitorum superficialis (FDS) and the flexor digitorum profundus (FDP) PCSAs. The PCSA values used in this paper are taken from Ref. [29] and summarized in Table 1. Different specific tension values have been reported in the literature (15 N/cm$^2$ [30], 22.5 N/cm$^2$ [31], 19–30 N/cm$^2$ [32], 35 N/cm$^2$ [29], 70 N/cm$^2$ [33], and 100 N/cm$^2$ [34]). For this study, an average specific tension value of 50 N/cm$^2$ has been used. Therefore, the maximum isometric muscle forces for the extensor and the flexor are calculated to be 102.5 N and 310.5 N, respectively.

(2) Anthropometric properties of the index finger, including length, mass, and moment of inertia are taken from Ref. [35]. The composite moment of inertia is calculated given the masses and moments of inertia of the three phalanges of the index finger.

(3) Muscle moment arms are assumed to be constant during the motion because of small finger rotation amplitude, and both radii are assumed to be 10 mm, which agrees with the dimensions of the metacarpophalangeal joint [36].

The dynamics of the index finger model can be summarized as follows:

$$\ddot{\theta} = \frac{1}{I}\left(mgd\cos(\theta) + r_f F_f - r_e F_e\right) \tag{1}$$

where $\theta$ is the index finger angle (positive in flexion direction), and $m$ and $d$ are the finger mass and the center of mass location, respectively. $r_f$ and $r_e$ are the flexor and extensor moment arms, which are multiplied by flexor and extensor muscle forces, $F_f$ and $F_e$, to produce the joint moments. The list of all the simulation parameters and their numerical values are listed in Table 2.

For the tapping motion, the desired joint angle is defined as follows:

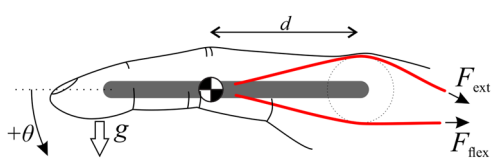


**Fig. 1 The schematic of the musculoskeletal finger model**

**Table 1 The physiological cross-sectional areas (PCSAs) of the index finger muscles from Ref. [29]**

| | Muscle | PCSA (cm$^2$) | Effective PCSA (cm$^2$) |
|---|---|---|---|
| Extensors | EDC-I[a] | 0.90 | 2.05 |
| | EIP | 1.15 | |
| Flexors | FDS-I[a] | 2.81 | 6.21 |
| | FDP-I[a] | 3.40 | |

[a]"I" represents the index finger portions of the muscle.

$$\theta_d(t) = 0.31\sin(\omega_d t) \tag{2}$$

where 0.31 rad ($\cong$ 18 deg) is the amplitude of the measured metacarpophalangeal joint motion during finger tapping [37], and $\omega_d = 2\pi f_d$, in which $f_d$ is the frequency of the sinusoidal motion.

The inputs to the simulations are the two muscle excitation signals. Provided the excitations are given, the equations of motion (Eqs. (1) and (A1)) are integrated forward in time to find the changes in finger kinematics.

## 3 Optimization Problem Description

To define the control signals through the course of the tapping motion, they are globally parametrized by seventh-order Fourier series

$$u = \frac{1}{2}A_0 + \sum_{n=1}^{7} A_n \cos\left(\frac{2\pi n t}{\tau_d} + B_n\right) \tag{3}$$

where $A_n$ and $B_n$ are the Fourier coefficients, and $\tau_d$ is the motion period. The major reason for assuming such a pattern is that filtered, rectified, and normalized electromyogram signals are quite smooth and can be curve-fitted by a suitable continuous mathematical function. Furthermore, a Fourier series function is periodic, making it an ideal choice for the simulation of the periodic finger tapping motion. Assuming a continuous and continuously differentiable function like a Fourier series will also help the optimizer to meet the nonlinear constraints on the excitation signal within the optimization problem definition. Finally, assuming a parametric continuous function may possibly lead to symbolic simplifications and analytical solutions.

Therefore, the optimizer job is to find the optimal coefficients of the two control signals, for a total of 30 variables (15 for each signal). A set of nonlinear constraints will be imposed to the problem to meet the bounds on the neural excitations, i.e., $0 \le u \le 1$.

The objective function for simulating this model is defined as a linear combination of two cost functions

$$J = \mu J_1 + (1-\mu)J_2 \tag{4}$$

where

$$J_1 = \frac{1}{N\tau_d}\sum_{j=1}^{2}\int_0^{N\tau_d} a_j^2\, dt \tag{5}$$

$$J_2 = \frac{1}{N\tau_d}\int_0^{N\tau_d}\left[\frac{\theta_s - \theta_d}{\max(\theta_d)}\right]^2 dt \tag{6}$$

Here, the first term, $J_1$, describes the physiological effort index based on Ref. [38], whereas the second term, $J_2$, accounts for the tracking error. In these equations, $\tau_d = 1/f_d$ is the desired motion period, and $N$ is the number of cycles simulated, which was set to be 3 to ensure periodicity of the motion in consecutive cycles; $j$ is the muscle index; $\theta_s$ and $\theta_d$ are the simulated and desired joint angles, respectively; and $\max(\theta_d)$ refers to amplitude of the



Downloaded From: http://computationalnonlinear.asmedigitalcollection.asme.org/ on 01/15/2018 Terms of Use: http://www.asme.org/about-asme/terms-of-use

**Table 2 List of simulation parameters**

| Parameter | Value |
|---|---|
| $I$ | $5.9 \times 10^{-4}$ kg m$^2$ |
| $m$ | $6.5 \times 10^{-2}$ kg |
| $d$ | $4.4 \times 10^{-2}$ m |
| $F_{\max,e}$ | 102.5 N |
| $F_{\max,f}$ | 310.5 N |
| $L_{ce}^{opt}$ | 0.178 m |
| $r_f$, $r_e$ | 0.01 m |

desired motion (=0.31 rad). The weight factor $\mu$ indicates the relative importance of the physiological term against the tracking error. Since in this simulation, tracking of the motion is much more important, the weight factor is assumed to be $\mu = 0.1$. It must be noted that the objective functional is written so that each term is dimensionless.

The optimization procedure was similar to that used in Refs. [17], [20], [25], [26], and [39]. In brief, sequential quadratic programming (SQP) as implemented in the fmincon function in the Optimization Toolbox of MATLAB® is used as the optimizer. For the initial guess needed in SQP, the results of the same case using a genetic algorithm as the optimizer were used. For more details on the optimization set up and the convergence criteria, refer to Refs. [17] and [25].

## 4 Results

Different sets of simulations were run. In the first set of simulations, the major focus was on the motion frequency variation. A separate set of simulations was also done on the effect of model parameters (e.g., finger mass) on the results.

Figure 2 shows how increasing the motion frequency affects the tracking capability of the model. As the purpose was to find the maximum frequency that this biomechanical system could follow, motion frequency started from 2 Hz (top row in Fig. 2) and was increased to 7.5 Hz in 0.5 Hz increments. The plots show $\theta_d$ and $\theta_s$ (desired and simulated motions), muscle excitations/activations and muscle forces (respectively, from left to right).

A separate study was also done to investigate the sensitivity of the simulation results to the finger mass. To this goal, finger mass and moment of inertia were reduced to 50%, and the optimal control problem was resolved for this case at $f_d = 2$ Hz. Optimal muscle excitations, activations, and forces of this case are shown in Fig. 3.

## 5 Discussion

The quantitative measures of tracking performance is shown in Fig. 4. It can be observed in Fig. 4(*b*) that the system was not able to fully track the desired motion after 6 Hz. Beyond this frequency, tracking performance worsened significantly (notice the nonlinear increase in the logarithmic scale in Fig. 4(*a*)), despite the monotonically increasing physiological effort.

At low frequencies (e.g., $f_d = 2$ Hz), the simulated and the desired motions are identical, resulting in a small value for $J_2$ (see Fig. 4(*a*)). Furthermore at this low frequency, the extensor activity is much higher than the flexor. This is due to the fact that the muscles are uni-articular (they span only one joint), and theoretically no co-activation should occur in the optimal results [40]. The results imply that at a low frequency, the gravity can produce enough flexion acceleration; thus, the flexor muscle has negligible activity.

As the motion frequency increases, the tracking performance decreases, which can be observed from the increased $J_2$ values in Fig. 4(*a*). This is due to the trade-off between the tracking error and the physiological effort (the physiological effort to produce faster motion increases).

An interesting phenomenon happens at about 6.5 Hz: the extensor muscle saturates (muscle excitation reaches the limit $u_{ext} = 1$). Higher than 6.5 Hz, due to muscle excitation saturation, it is impossible to fully track the desired motion; therefore, the tracking error increases significantly (note the change in the slope of the tracking error curve in Fig. 4(*a*)). Furthermore, the ratio of the tracking error to the total cost function value shows significant changes after 6 Hz (Fig. 4(*b*)), which also demonstrates the inability to follow the desired motion.

There are a number of studies in the literature on finding the maximal frequency or speed at which a finger can move. Kuboyama et al. mentioned $6.46 \pm 0.72$ Hz in Ref. [41] and $6.6 \pm 0.9$ Hz in Ref. [42], while Aoki and Fukuoka [43] reported 160 ms intertap interval (=6.25 Hz). The results of this study imply that this maximal frequency is approximately 6 Hz, which is close to the available values in the literature. These mentioned references have measured the desired value experimentally, so the maximal motion frequency extracted from the results of this study predicts the experiments reasonably well.

Multiple phenomena may contribute to the inability of the finger to follow the desired trajectory. The excitation/activation coupling model causes a time delay between neural excitation and activation signals, as well as a nonlinearity and scaling imposition between these two signals [44]. These dynamics can be an important cause of the inability to follow fast oscillations. Figure 5 shows the signal attenuation due to the excitation/activation dynamics. To obtain this response, sinusoidal excitation inputs were applied, and the ratio of the amplitudes of the muscle activation and excitation signals (i.e., $\mathrm{amp}(a(t))/\mathrm{amp}(u(t))$) was calculated after the transient response vanished. As can be seen, the excitation/activation dynamics essentially performs as a low-pass filter with a bandwidth of ~4.5 Hz (defined as 3 dB amplitude attenuation). At 6 Hz, the amplitude attenuation is 4 dB; i.e., the amplitude of the activation signal is 63% of that of the excitation.

The attenuation of the activation signal amplitude is exacerbated by the muscle properties. A muscle's force production capacity drops as the muscle contraction velocity increases (see Fig. 6). At high motion frequencies, the required contraction velocity is more than the velocity at which the muscle can produce the force to satisfy the equations of motion. Figure 6, which shows the force–length–velocity relationship, implies that when the concentric contraction velocity increases, the force production ability decreases. Therefore, the muscle can move faster only if it can produce enough force to satisfy the equations of motion. At around 6 Hz, the muscle must contract with the maximum shortening velocity of $-117$ mm/s ($= -0.66\,\mathrm{s}^{-1}$ when normalized to muscle fiber length), which along with the filtering effect, will lead to small force generation ability. Since the muscle cannot create enough force at such a velocity in order to satisfy the equations of motion, it is not able to sufficiently contract at this velocity.

As discussed earlier, the inability to follow the requested frequency of the sinusoidal motion is due to the saturation of the extensor, which can be related to the reduced muscle force capacity at the given velocity. However, this proportionally depends on the chosen values of the $F_{\max}$ for the extensor muscle group in the Hill muscle model. As there was a broad range reported for the muscle specific strength and we picked 50 N/cm$^2$, the findings of this study would depend on the chosen specific tension. Therefore, from the musculoskeletal modeling perspective, the maximum tapping frequency depends on the muscle specific tension, which might be a limitation for our simulation framework.

The amplitude of the adopted motion can also affect the maximum tapping frequency. By lowering the amplitude of the motion, the motion becomes less demanding, and the musculotendon velocities are decreased, which may increase the model's prediction for the maximum achievable frequency. We observed that a higher frequency can be reached using a smaller motion amplitude



Downloaded From: http://computationalnonlinear.asmedigitalcollection.asme.org/ on 01/15/2018 Terms of Use: http://www.asme.org/about-asme/terms-of-use

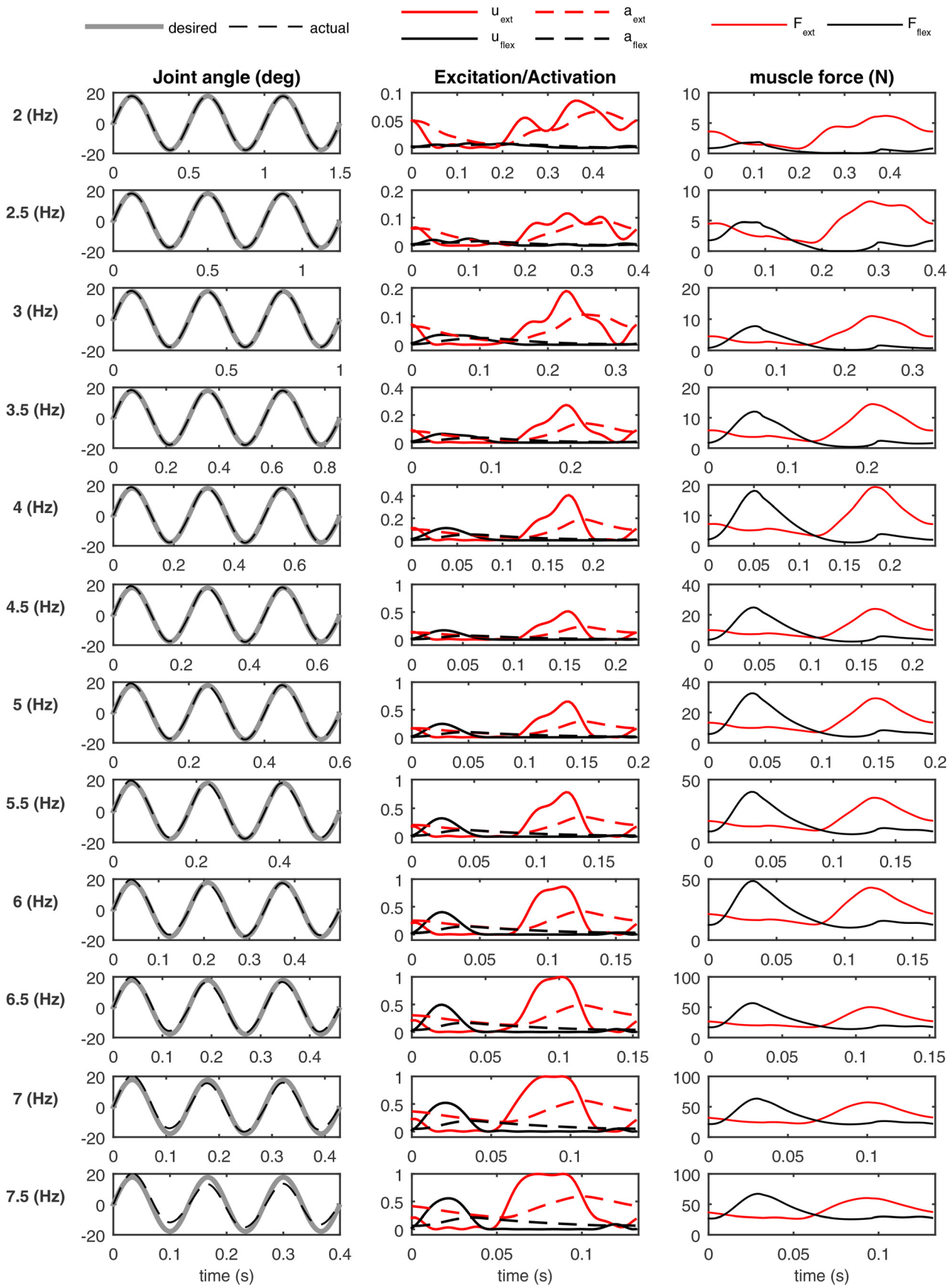


**Fig. 2 The simulation results for different frequencies. The columns from left to right show: the desired and simulated joint angle trajectories, flexor/extensor muscle excitation and activation, and flexor/extensor muscle force. To provide more clarity, muscle results are shown for one period only.**



**Downloaded From: http://computationalnonlinear.asmedigitalcollection.asme.org/ on 01/15/2018 Terms of Use: http://www.asme.org/about-asme/terms-of-use**

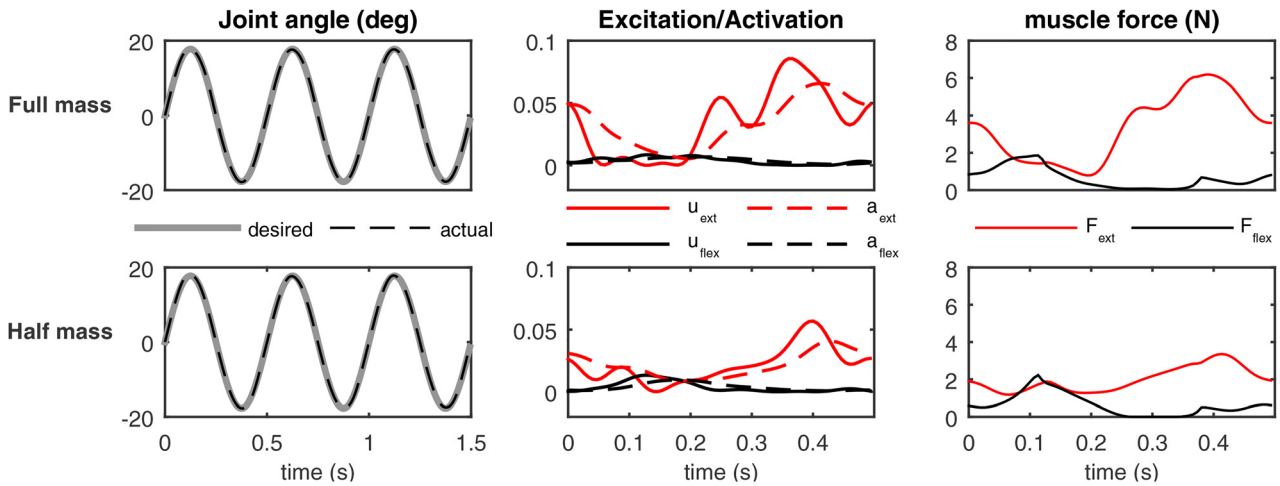


**Fig. 3 (*a*) Variation of motion frequency and cost function values and (*b*) the ratio of the tracking error term to the total cost function value**

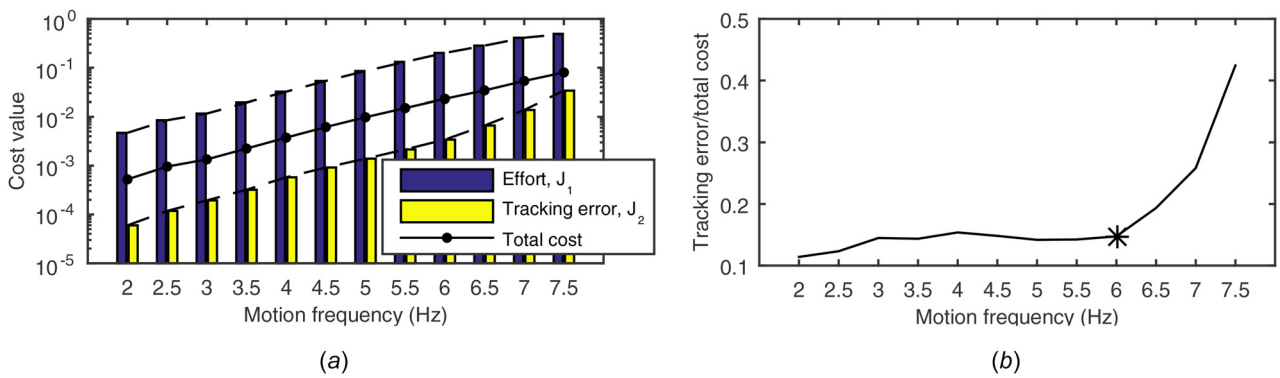


**Fig. 4 Optimal results for $f_d = 2$ Hz and 50% of index finger mass; from left to right: joint angle trajectories, muscle excitation/activations, and muscle force. To provide more clarity, muscle results are shown for one period only.**

(up to about 7.5 Hz with 0.25% amplitude, i.e., about 4 deg). However, at such higher frequencies, the limiting factor is no longer the saturation of the excitation signal ($u = 1$). Instead, the excitation/activation dynamics is the bottleneck, which essentially filters the high-frequency excitation signal and restricts the required rate of force production. Furthermore, at those high frequencies, simulations show high antagonistic co-contraction that is the result of the insufficient time for the muscles to relax. Because of this issue, we observed that further reduction in oscillation amplitude does not increase the maximum achievable frequency. Therefore, one can argue that even if the muscles are strong enough to produce as much force as necessary, there is still a definite upper limit for how fast the finger can move, which is due to the dynamics of the excitation/activation coupling.

Comparing the results of the model with 50% mass and moment of inertia (Fig. 3) with the same case in Fig. 2 (top row, $f_d = 2$ Hz) shows that the quality of the motion tracking is the same, but the

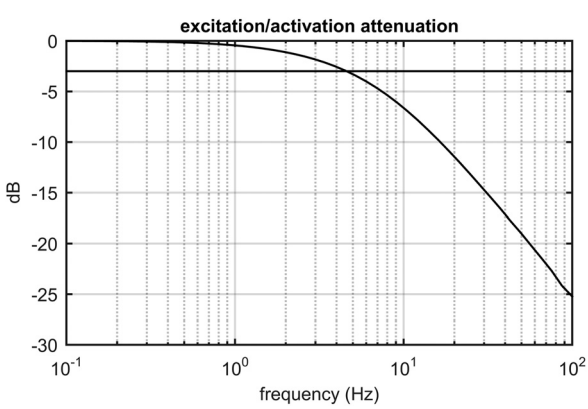


**Fig. 5 The frequency response of the excitation/activation dynamics. The dynamics perform similar to a low-pass filer with a bandwidth of about 4 Hz. Thus, the activation signal amplitude drops at high frequencies.**

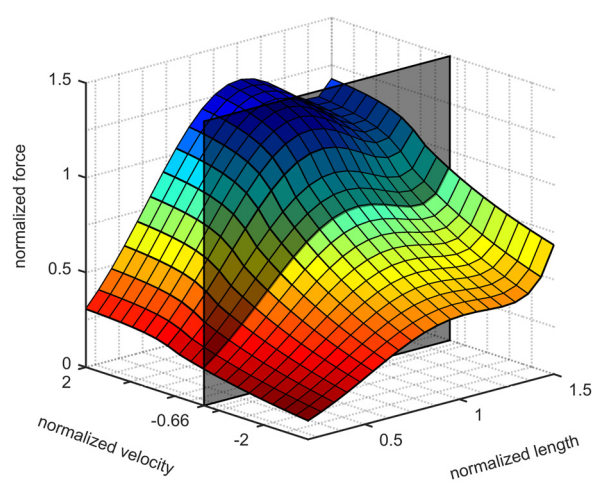


**Fig. 6 The force–length–velocity relation in the muscle model**



Downloaded From: http://computationalnonlinear.asmedigitalcollection.asme.org/ on 01/15/2018 Terms of Use: http://www.asme.org/about-asme/terms-of-use

excitation values in the case with 50% mass is roughly half the original values. This is reasonable since the dominant term in the dynamics of the finger is the inertia. Moreover, the motion velocity is not high enough to significantly affect the force–velocity relation. The simulation with altered finger mass showed that the modeling framework is able to simulate the system response even with a large change in model mass. This is a necessary feature for subject-specific simulations. With a more detailed sensitivity analysis, we can investigate the effects of parameters on the system dynamics, as well as the intended outcomes. For example, including contact dynamics (e.g., volumetric technique as in Refs. [45] and [46]) in the musculoskeletal models can allow for design optimization of musical instruments, such as the piano keys, or enhance the ergonomics of computer keyboards.

The goal of this study was to target oscillatory tapping motions. Since the human motions are smooth unless they are imposed to impulses from external sources, sinusoidal patterns seem to be a reasonable choice for the designed task. However, to study the maximum frequency of index finger movement in general, other trajectories such as smooth step functions may also be investigated.

## 6 Conclusions

In this study, we presented a musculoskeletal modeling framework to study the fast finger tapping motion. The forward dynamics simulations showed that the maximum achievable motion frequency was roughly 6 Hz, matching experimental observations. We have made arguments that the limiting factor in this case was the excitation/activation filtering effect, as well as the inability of muscles to produce enough force at high contractile velocities.


## Acknowledgment

The authors wish to acknowledge the Natural Sciences and Engineering Research Council of Canada (NSERC) for funding support of this study.


## Appendix: Thelen's Muscle Model Formulation

### Excitation/Activation Dynamics

The excitation/activation dynamics is described as [28]

$$\dot{a}(t) = \frac{u - a}{\tau(u, a)} \tag{A1}$$

where

$$\tau(u, a) = \begin{cases} t_1 \hat{a} & u \geq a \\ t_2 / \hat{a} & u < a \end{cases} \tag{A2}$$

and

$$\hat{a} = 0.5 + 1.5a \tag{A3}$$

The parameter values of $t_1 = 15\,\text{ms}$ and $t_2 = 50\,\text{ms}$ are taken from Ref. [28].

### Tendon Force

The tendon force is normalized to muscle maximum isometric force $F_{\max}$ and is represented as an exponential function of the tendon strain

$$\tilde{f}^t = \begin{cases} \dfrac{\tilde{f}^t_{\text{toe}}}{e^{k_{\text{toe}}} - 1}\left(e^{\frac{k_{\text{toe}}\varepsilon^t}{\varepsilon^t_{\text{toe}}}} - 1\right) & \varepsilon^t \leq \varepsilon^t_{\text{toe}} \\ k_{\text{lin}}\left(\varepsilon^t - \varepsilon^t_{\text{toe}}\right) + \tilde{f}^t_{\text{toe}} & \varepsilon^t > \varepsilon^t_{\text{toe}} \end{cases} \tag{A4}$$

where $\varepsilon^t$ is the engineering strain of tendon (calculated based on the slack length $l_{\text{slack}}$), $\varepsilon^t_{\text{toe}}$ is a limit after which the tendon relation switches to the linear expression, $k_{\text{toe}}$ is a shape factor, $k_{\text{lin}}$ is the linear slope of the second condition, and $\tilde{f}^t_{\text{toe}}$ is the function value at $\varepsilon^t = \varepsilon^t_{\text{toe}}$. Values of the parameters are adopted from Ref. [28]: $k_{\text{toe}} = 3, \tilde{f}^t_{\text{toe}} = 0.33, \varepsilon^t_0 = 0.04, \varepsilon^t_{\text{toe}} = 0.609\varepsilon^t_0$, and $k_{\text{lin}} = 1.712/\varepsilon^t_0$.

### Parallel Elastic Element

The relation for muscle passive force normalized to muscle maximum isometric force $F_{\max}$ is expressed as

$$\tilde{f}^{\text{pe}} = \frac{e^{\frac{k^{\text{pe}}\left(\tilde{l}\,\text{ce} - 1\right)}{\varepsilon^m_0}} - 1}{e^{k^{\text{pe}}} - 1} \tag{A5}$$

where $\tilde{l}^{\text{ce}}$ is the muscle fiber length normalized to $l^{\text{ce}}_{\text{opt}}$, $k^{\text{pe}}$ is a shape parameter set to 5, and $\varepsilon^m_0$ is called the passive muscle strain and adopted to be 0.6 (for young adults).

### Force–Length–Velocity Relation

The force–length relation is written as

$$f^{\text{ce}}_{\text{isom}} = e^{-\frac{(\tilde{l}^{\text{ce}} - 1)^2}{\gamma}} \tag{A6}$$

where $\gamma$ is a shape factor and is set to be 0.45.

Afterward, the total force–length–velocity in this muscle model can be formulated as the following:

$$v^{\text{ce}} = (0.25 + 0.75a)\, v^{\text{ce}}_{\max} \frac{\tilde{f}^{\text{ce}} - a f^{\text{ce}}_{\text{isom}}}{b} \tag{A7}$$

where

$$b = \begin{cases} a f^{\text{ce}}_{\text{isom}} + \tilde{f}^{\text{ce}}/A_f & \tilde{f}^{\text{ce}} \leq a f^{\text{ce}}_{\text{isom}} \\ \dfrac{(2 + 2/A_f)\left(a f^{\text{ce}}_{\text{isom}}\hat{f} - \tilde{f}^{\text{ce}}\right)}{\hat{f} - 1} & \tilde{f}^{\text{ce}} > a f^{\text{ce}}_{\text{isom}} \end{cases} \tag{A8}$$

Here, $v^{\text{ce}}$ is the fiber velocity (velocity of the contractile element, CE), $\tilde{f}^{\text{ce}}$ is the force of CE element normalized to maximum isometric force, $\hat{f}$ is the normalized asymptotic eccentric force (equal to 1.4 for young adults), $A_f$ is a shape parameter (adopted to be 0.25), and $v^{\text{ce}}_{\max} = 10\, l^{\text{ce}}_{\text{opt}}\,\text{m/s}$ is the maximum contraction velocity of the muscle fiber.

## References


[1] Wu, J. Z., An, K.-N., Cutlip, R. G., Krajnak, K., Welcome, D., and Dong, R. G., 2008, "Analysis of Musculoskeletal Loading in an Index Finger During Tapping," J. Biomech., **41**(3), pp. 668–676.

[2] Brook, N., Mizrahi, J., Shoham, M., and Dayan, J., 1995, "A Biomechanical Model of Index Finger Dynamics," Med. Eng. Phys., **17**(1), pp. 54–63.

[3] Kirk, D. E., 2004, *Optimal Control Theory: An Introduction*, Dover Publications, Mineola, New York.

[4] Betts, J., 2001, *Practical Methods for Optimal Control Using Nonlinear Programming*, SIAM, Philadelphia, PA.

[5] Chachuat, B. C., 2007, *Nonlinear and Dynamic Optimization: From Theory to Practice*, Automatic Control Laboratory, EPFL, Lausanne, Switzerland.

[6] Sharif Razavian, R., Mehrabi, N., and McPhee, J., 2015, "A Model-Based Approach to Predict Muscle Synergies Using Optimization: Application to Feedback Control," Front. Comput. Neurosci., **9**, pp. 1–13.

[7] Ackermann, M., and van den Bogert, A. J., 2010, "Optimality Principles for Model-Based Prediction of Human Gait," J. Biomech., **43**(6), pp. 1055–1060.





Downloaded From: http://computationalnonlinear.asmedigitalcollection.asme.org/ on 01/15/2018 Terms of Use: http://www.asme.org/about-asme/terms-of-use

[8] de Groote, F., Kinney, A. L., Rao, A. V., and Fregly, B. J., 2016, "Evaluation of Direct Collocation Optimal Control Problem Formulations for Solving the Muscle Redundancy Problem," Ann. Biomed. Eng., **44**(10), pp. 2922–2936.
[9] Meyer, A., Eskinazi, I., Jackson, J., Rao, A., Patten, C., and Fregly, B., 2016, "Muscle Synergies Facilitate Computational Prediction of Subject-Specific Walking Motions," Front. Bioeng. Biotechnol, **4**, p. 77.
[10] Todorov, E., and Jordan, M. I., 2002, "Optimal Feedback Control as a Theory of Motor Coordination," Nat. Neurosci., **5**(11), pp. 1226–1235.
[11] Todorov, E., 2004, "Optimality Principles in Sensorimotor Control," Nat. Neurosci., **7**(9), pp. 907–915.
[12] Li, W., and Todorov, E., 2004, "Iterative Linear Quadratic Regulator Design for Nonlinear Biological Movement Systems," 1st International Conference on Informatics in Control, Automation and Robotics (ICINCO), Setúbal, Portugal, Aug. 25–28, pp. 1–8.
[13] Liu, D., and Todorov, E., 2009, "Hierarchical Optimal Control of a 7-DOF Arm Model," IEEE Symposium on Adaptive Dynamic Programming and Reinforcement Learning (ADPRL), Nashville, TN, Mar. 30–Apr. 2, pp. 50–57.
[14] Rao, A. V., 2009, "A Survey of Numerical Methods for Optimal Control," Adv. Astronaut. Sci., **135**(1), pp. 497–528.
[15] Ackermann, M., 2007, "Dynamics and Energetics of Walking With Prostheses," Ph.D. thesis, University of Stuttgart, Stuttgart, Germany.
[16] Anderson, F. C., and Pandy, M. G., 2001, "Dynamic Optimization of Human Walking," ASME J. Biomech. Eng., **123**(5), pp. 381–390.
[17] Shourijeh, M. S., and McPhee, J., 2014, "Optimal Control and Forward Dynamics of Human Periodic Motions Using Fourier Series for Muscle Excitation Patterns," ASME J. Comput. Nonlinear Dyn., **9**(2), p. 021005.
[18] Rasmussen, J., Damsgaard, M., and Voigt, M., 2001, "Muscle Recruitment by the Min/Max Criterion—A Comparative Numerical Study," J. Biomech., **34**(3), pp. 409–415.
[19] Shourijeh, M. S., Mehrabi, N., and McPhee, J., 2017, "Forward Static Optimization in Dynamic Simulation of Human Musculoskeletal Systems: A Proof-of-Concept Study," ASME J. Comput. Nonlinear Dyn., epub.
[20] Shourijeh, M. S., Smale, K. B., Potvin, B. M., and Benoit, D. L., 2016, "A Forward-Muscular Inverse-Skeletal Dynamics Framework for Human Musculoskeletal Simulations," J. Biomech., **49**(9), pp. 1718–1723.
[21] Mehrabi, N., Sharif Razavian, R., and McPhee, J., 2015, "Steering Disturbance Rejection Using a Physics-Based Neuromusculoskeletal Driver Model," Veh. Syst. Dyn., **53**(10), pp. 1393–1415.
[22] Mehrabi, N., Sharif Razavian, R., and McPhee, J., 2015, "A Physics-Based Musculoskeletal Driver Model to Study Steering Tasks," ASME J. Comput. Nonlinear Dyn., **10**(2), p. 021012.
[23] Mehrabi, N., Sharif Razavian, R., and McPhee, J., 2013, "A Three-Dimensional Musculoskeletal Driver Model to Study Steering Tasks," ASME Paper No. DETC2013-13101.
[24] Garcia-Vallejo, D., and Schiehlen, W., 2012, "3D-Simulation of Human Walking by Parameter Optimization," Arch. Appl. Mech., **82**(4), pp. 533–556.
[25] Shourijeh, M. S., and McPhee, J., 2014, "Forward Dynamic Optimization of Human Gait Simulations: A Global Parameterization Approach," ASME J. Comput. Nonlinear Dyn., **9**(3), p. 031018.
[26] Sharif Razavian, R., Mehrabi, N., and McPhee, J., 2015, "A Neuronal Model of Central Pattern Generator to Account for Natural Motion Variation," ASME J. Comput. Nonlinear Dyn., **11**(2), p. 021007.
[27] Sharif Razavian, R., and McPhee, J., 2015, "Minimization of Muscle Fatigue as the Criterion to Solve Muscle Forces-Sharing Problem," ASME Paper No. DSCC2015-9678.
[28] Thelen, D. G., 2003, "Adjustment of Muscle Mechanics Model Parameters to Simulate Dynamic Contractions in Older Adults," ASME J. Biomech. Eng., **125**(1), pp. 70–77.
[29] Keir, P. J., 1995, "Functional Implications of the Musculoskeletal Anatomy and Passive Tissue Properties of the Forearm," Ph.D. thesis, University of Waterloo, Waterloo, ON, Canada.
[30] Maganaris, C. N., Baltzopoulos, V., Ball, D., and Sargeant, A. J., 2001, "In Vivo Specific Tension of Human Skeletal Muscle," J. Appl. Physiol., **90**(3), pp. 865–872.
[31] Powell, P. L., Roy, R. R., Kanim, P., Bello, M. A., and Edgerton, V. R., 1984, "Predictability of Skeletal Muscle Tension From Architectural Determinations in Guinea Pig Hindlimbs," J. Appl. Physiol., **57**(6), pp. 1715–1721.
[32] Bárány, M., and Close, R. I., 1971, "The Transformation of Myosin in Cross-Innervated Rat Muscles," J. Physiol., **213**(2), pp. 455–474.
[33] Kawakami, Y., Nakazawa, K., Fujimoto, T., Nozaki, D., Miyashita, M., and Fukunaga, T., 1994, "Specific Tension of Elbow Flexor and Extensor Muscles Based on Magnetic Resonance Imaging," Eur. J. Appl. Physiol. Occup. Physiol., **68**(2), pp. 139–47.
[34] An, K. N., Kaufman, K. R., and Chao, E. Y. S., 1989, "Physiological Considerations of Muscle Force Through the Elbow Joint," J. Biomech., **22**(11–12), pp. 1249–1256.
[35] Buchner, H. M., and Hemami, H., 1988, "A Dynamic Model for Finger Interphalangeal Coordination," J. Biomech., **21**(6), pp. 459–468.
[36] Unsworth, A., and Alexander, W. J., 1979, "Dimensions of the Metacarpophalangeal Joint With Particular Reference to Joint Prostheses," Eng. Med., **8**(2), pp. 75–80.
[37] Kuo, P. L., Lee, D. L., Jindrich, D. L., and Dennerlein, J. T., 2006, "Finger Joint Coordination During Tapping," J. Biomech., **39**(16), pp. 2934–2942.
[38] Happee, R., 1994, "Inverse Dynamic Optimization Including Muscular Dynamics, a New Simulation Method Applied to Goal Directed Movements," J. Biomech., **27**(7), pp. 953–960.
[39] Shourijeh, M. S., 2013, "Optimal Control and Multibody Dynamic Modelling of Human Musculoskeletal Systems," Ph.D. thesis, University of Waterloo, Waterloo, ON, Canada.
[40] Kerwin, J., and Challis, D., 1993, "An Analytical Examination of Muscle Force Estimations Using Optimization Techniques," J. Eng. Med., **207**(3), pp. 139–148.
[41] Kuboyama, N., Nabetani, N., Shibuya, K., Machida, K., and Ogaki, T., 2004, "The Effect of Maximal Finger Tapping on Cerebral Activation," J. Physiol. Anthropol. Appl. Hum. Sci., **23**(4), pp. 105–110.
[42] Kuboyama, N., Nabetani, T., Shibuya, K., Machida, K., and Ogaki, T., 2005, "Relationship Between Cerebral Activity and Movement Frequency of Maximal Finger Tapping," J. Physiol. Anthropol. Appl. Hum. Sci., **24**(3), pp. 201–208.
[43] Aoki, T., and Fukuoka, Y., 2010, "Finger Tapping Ability in Healthy Elderly and Young Adults," Med. Sci. Sports Exercise, **42**(3), pp. 449–455.
[44] He, J., Levine, W. S., and Loeb, G. E., 1991, "Feedback Gains for Correcting Small Perturbations to Standing Posture," IEEE Trans. Auton. Control, **36**(3), pp. 322–332.
[45] Shourijeh, M. S., and McPhee, J., 2013, "Efficient Hyper-Volumetric Contact Dynamic Modelling of the Foot Within Human Gait Simulations," ASME Paper No. DETC2013-13446.
[46] Shourijeh, M. S., and McPhee, J., 2015, "Foot–Ground Contact Modeling Within Human Gait Simulations: From Kelvin–Voigt to Hyper-Volumetric Models," Multibody Syst. Dyn., **35**(4), pp. 393–407.



**Downloaded From: http://computationalnonlinear.asmedigitalcollection.asme.org/ on 01/15/2018 Terms of Use: http://www.asme.org/about-asme/terms-of-use**